RESEARCH ARTICLE

Barbigerone Inhibits Tumor Angiogenesis, Growth and Metastasis in Melanoma

Jian-Hong Yang[1], Jia Hu[1], Li Wan[2]*, Li-Juan Chen[1]*

Abstract

   Tumor angiogenesis, growth and metastasis are three closely related processes. We therefore investigated the effects of barbigerone on all three in the B16F10 tumor model established in both zebrafish and mouse models, and explored underlying molecular mechanisms. *In vitro*, barbigerone inhibited B16F10 cell proliferation, survival, migration and invasion and suppressed human umbilical vascular endothelial cell migration, invasion and tube formation in concentration-dependent manners. In the transgenic zebrafish model, treatment with 10µM barbigerone remarkably inhibited angiogenesis and tumor-associated angiogenesis by reducing blood vessel development more than 90%. *In vivo*, barbigerone significantly suppressed angiogenesis as measured by H and E staining of matrigel plugs and CD31 staining of B16F10 melanoma tumors in C57BL/6 mice. Furthermore, it exhibited highly potent activity at inhibiting tumor growth and metastasis to the lung of B16F10 melanoma cells injected into C57BL/6 mice. Western blotting revealed that barbigerone inhibited phosphorylation of AKT, FAK and MAPK family members, including ERK, JNK, and p38 MAPKs, in B16F10 cells mainly through the MEK3/6/p38 MAPK signaling pathway. These findings suggested for the first time that barbigerone could inhibit tumor-angiogenesis, tumor growth and lung metastasis via downregulation of the MEK3/6/p38 MAPK signaling pathway. The findings support further investigation of barbigerone as a potential anti-cancer drug.

Keywords: Barbigerone - metastasis - angiogenesis - p38 MAP kinase - melanoma cancer

Introduction

   Tumor cells are characterized by uncontrolled growth, invasion to surrounding tissues, and metastatic spread to distant sites. Tumor angiogenesis, tumor growth and tumor metastasis are three closely related processes. Tumor angiogenesis, the development of new blood vessels from the existing vasculature, is considered a critical event in tumor growth and metastasis because when tumor grows beyond 2 to 3 mm it requires the formation of new blood vessels to provide essential nutrients, oxygen and metastatic passageway for tumors (Folkman, 1971; Folkman et al., 1992; Carmeliet et al., 2000; Carmeliet, 2003; Ferrara et al., 2005; Carmeliet et al., 2008).

   The mitogen-activated protein kinase (MAPK) signaling pathways play essential roles in cell survival, proliferation and migration. MAPK pathway is relevant to human carcinogenesis (Amundadottir et al., 1998; Webb et al., 1998; Reddy et al., 2003). They are the major players to mediate a variety of signals for cellular functions (Johnson et al., 2002). In addition, activation of ERK has been observed in a number of tumors (Vicent et al., 2004). Activation of c-jun-NH2-kinase and p38 has been found in prostate carcinoma (Uzgare et al., 2003)

and breast carcinoma (Davidson et al., 2006). Recent studies have shown the activation of MAPK signaling pathways including extracellular signal-regulated protein kinase (ERK), c-Jun amino-terminal kinases (JNK), and p38 MAPK (p38) in tumorigenesis, metastasis, and angiogenesis of multiple human malignancies (Huang et al., 2008).

   Barbigerone (Figure 1A), a naturally occurring isoflavone, formally named as 2', 4', 5'-trimethoxy-6'', 6''-dimethylpyrano (2'', 3'': 7, 8) isoflavone, was first isolated from the seeds of Tephrosia barbigera in 1979 (Vilain, 1980) and found with minor content in species of Milletia of Leguminosae family and species of Satcolobus of Asclepiadaceae family (Yenesew et al., 1998; Wangensteen et al., 2005). This compound has exhibited profound pharmacological properties, such as antioxidant, 15-lipoxygenase inhibitory activity (Wangensteen et al., 2006), and anti-plasmodial activity (Yenesew et al., 2003). Our previous study has shown that BA exhibited antitumor activity on murine and human cancer cells by inducing apoptosis (Li et al., 2010), and inhibits tumor angiogenesis and human non-small-cell lung cancer xenografts growth through VEGFR2 signaling pathways (Li et al., 2012). In this study, we investigated the effects of barbigerone on

*[1]Department of Medical Oncology, Cancer Center, State Key Laboratory of Biotherapy, West China Hospital, West China Medical School, Sichuan University, [2]State Key Laboratory Breeding Base of Systematic Research, Development and Utilization of Chinese Medicine, The Ministry of Education Key Laboratory of Standardization of Chinese Herbal Medicine, Chengdu University of Traditional Chinese Medicine, Chengdu, China *For correspondence: chenlijuan125@163.com, wanli8801@163.com*

tumor angiogenesis, tumor growth and metastasis in the B16F10 tumor model established on both zebrafish and mice models, and the underlying molecular mechanisms. We demonstrated that barbigerone significantly inhibited B16F10 tumor cells and endothelial cells proliferation, migration, invasion and tube formation. Barbigerone significantly suppressed tumor-angiogenesis, tumor growth and lung metastasis. Our cellular study showed that barbigerone could inhibit phosphorylation of MAPK family including ERK, JNK, and p38 MAPKs in B16F10 cells. The further investigation showed that barbigerone could strongly suppress the activity of both upstream factor phospho-MKK3/MKK6 and downstream factor phospho-MAPKAPK-2 in p38 signaling pathway. We demonstrate for the first time that barbigerone can inhibit tumor-angiogenesis, tumor growth and lung metastasis via downregulation of MEK3/6/p38 MAPK signaling pathway.

Materials and Methods

Reagents, cell line and cell culture

MTT (3-(4,5-dimethylthiazol-2-yl)-2, 5-diphenyltetrazolium bromide), dimethyl sulfoxide (DMSO), Hoechst33258, FITC-phalloidin and gelatin were purchase from Sigma Chemical Co. (St. Louis, MO). Matrigel was abtained from BD Biosciences. Anti-p44/42 MAP Kinase monoclonal rabbit antibody, anti-phospho-p44/42 MAP Kinase monoclonal rabbit antibody, anti-AKT monoclonal rabbit antibody, anti-phospho-AKT monoclonal rabbit antibody, anti-p38 MAP Kinase monoclonal rabbit antibody, anti-Phospho-p38 MAP Kinase monoclonal rabbit antibody, anti-JNK MAP Kinase monoclonal rabbit antibody, anti-phospho-JNK MAP Kinase monoclonal rabbit antibody, anti-FAK monoclonal rabbit antibody, anti-phospho-FAK monoclonal rabbit antibody, anti-Phospho-MKK3/MKK6 monoclonal rabbit antibody, anti-Phospho-MAPKAPK-2 monoclonal rabbit antibody and anti-Phospho-ATF-2 monoclonal rabbit antibody were purchased from Cell Signaling Laboratories (Beverly, MA); Anti-β-actin monoclonal mouse antibody, mouse anti-rabbit IgG/HRP and goat anti-mouse IgG/HRP were purchased from Santa Cruz Biotechnology (Santa Cruz, CA). The protein assay kit was obtained from Bio-Rad (Hercules, CA).

Barbigerone was isolated from Millettia pachycarpa Benth according to the protocols reported previously (Ye et al., 2010) with slight modifications. Samples containing 99% or higher barbigerone were used in all experiments unless otherwise indicated. Barbigerone was dissolved in DMSO as a stock solution and stored at 4ºC. Prior to experiment, the stock solution was diluted in cell-culture medium at final DMSO concentration of 0.05% (V/V). Controls were always treated with the same amount of DMSO as used in the corresponding experiment.

B16F10 cells and human umbilical vascular endothelial cells (HUVEC) were obtained from the American Type Culture Collection (ATCC) and incubated in DMEM containing 10% fetal bovine serum (FBS), 100 units/mL penicillin, and 100 μg/mL streptomycin. Cells were incubated at 37°C in a humidified atmosphere of 5 % CO_2.

Cell proliferation assay

Cell growth-inhibitory activities of barbigerone on B16F10 cells were evaluated by MTT assay. B16F10 cells were seeded in 96-well plate at a plating density of 0.5×10^4/mL, and cultured for 24 h. After 24 h, cells were exposed to barbigerone at various concentrations (0, 0.625 μM, 1.25 μM, 2.5 μM, 5 μM, 10 μM and 20 μM) in fresh DMEM medium. Barbigerone was dissolved in DMSO (the final concentration of DMSO did not exceed 0.05%). Four replicate wells for each treatment dose were performed. The plate was placed at 37°C in 5% CO_2 for various time points (24 h, 48 h and 72 h), and then 20 μL MTT (5 mg/mL) were added into the cells and incubated for 3 h at 37°C. After incubation, the supernatant was removed, the plates were re-added with 0.15 ml of DMSO, and the absorbance was measured at 570 nm by the Spectramax M5 Microtiter Plate Luminometer (Molecular Devices, USA). Absorbance of untreated cells was considered as 100%.

Morphological analysis of apoptosis

Apoptosis cells treated with barbigerone was measured by hoechst staining. B16F10 cells were seeded in 6 well plates at the density of 5×10^4/well and cultured for 24 h, followed by barbigerone treatment for 48 h. After fixation with 1 ml 4% paraformaldehyde for 20 min, cells were incubated with 1ml PBS containing 10 μg/mL hoechst33258 at room temperature for 10min in the dark. Then images were taken using inverted fluorescence microscopy (Olympus, Tokyo, Japan).

Wound-healing assay

We used an *in vitro* wound healing assay to assess cell migration. B16F10 cells and HUVECs were seeded at a plating density of 2×10^5 per well in 6-well plates which had been coated with 1% gelatin, cells grown in DMEM medium with 10% FBS overnight. After reaching 100% confluence, the cells were then gently scraped with a plastic tip to produce a wound area. After wounding cells were incubated with fresh DMEM medium with different doses (0, 1.25 μM, 2.5 μM, 5 μM) of barbigerone, the migration and cell movement throughout the wound area was examined after 24 h.

F-actin staining

Cells were grown on coverslips in DMEM medium with 10% fetal bovine containing 5μM barbigerone for 24h. After removing DMEM medium cells were fixed with 1ml 4% formaldehyde and stained with FITC-phalloidin for 30min in the dark. F-actin stress fibers were observed using inverted fluorescence microscopy (Olympus, Tokyo, Japan).

Transwell invasion assay

The 8μm transwell chambers were coated with Matrigel (BD Biosciences) and incubated in 24 well plates at 37°C for 30 min. The bottom chambers were filled with 600 μL DMEM medium with 10% fetal bovine serum and the top chambers were added 100 μL DMEM medium with 0.05% BSA and HUVEC or B16F10 (5×10^4 per well). The top and bottom chambers contained the same doses

of concentration of barbigerone (0, 1.25 μM, 2.5 μM, 5 μM). Cells were allowed to migrate for 16 h at 37°C, 5% CO_2. After the incubation, cells on the top surface of the membrane (non-migration) were scraped with a cotton swab. Cells on the bottom side of the membrane (migrated cells) were fixed with 1ml 4% paraformaldehyde for 20 min and washed three times with PBS. The cells were stained by crystal violet and then destained with PBS. The membranes were left to air dry and images were taken using inverted fluorescence microscopy (Olympus, Tokyo, Japan). Three independent areas per well were counted and the mean number of migrated cells was calculated.

Tube formation assay

To assess the tube-forming ability of HUVECs, a 96-microwell plate pre-chilled at 4°C, was carefully filled with 50 μL/well of liquid Matrigel (10 mg/ml) at 4°C with a pre-chilled pipette, avoiding bubbles. The Matrigel was polymerized for 1 h at 37°C, and HUVECs (20000 cells/well) were suspended in regular medium in the absence or presence of different concentrations (0, 1.25 μM, 2.5 μM, 5 μM) of barbigerone and carefully layered on the top of polymerized Matrigel. All tube formation experiments were observed using inverted fluorescence microscopy (Olympus, Tokyo, Japan), and images were digitally captured at 6 hour after plating.

Western blot

Total proteins were extracted for Western blot analyses in order to determine the expression levels of related proteins. B16F10 cells were cultured in 15-cm Petri dishes. After cells reaching 80% fusion, the cells were treated with various concentrations of barbigerone, and then incubated at 37°C. After 16 h, cells were lysed with protein lysis buffer. Western blot was performed as previously describe.

Zebrafish model

Zebrafish model was established as previously described (Zhao et al., 2011). In the first experiment, doses of barbigerone were added into the culture fluid of Flk-1-GFP transgenic zebrafish embryo at 10 hours post-fertilization (hpf). Pictures of trunk intersomite vessels and dorsal longitudinal anastomotic vessels were taken at 30 hpf.

In the second study, B16F10 cells were suspended in serum free DMEM medium and injected in the perivitelline space at 72 hpf. After divided into three groups randomly (n=30 per group) at 96 hpf, each group were treated with or without barbigerone. Observation of tumor induced angiogenesis was continued until 216 hpf. Photographs were taken under fluorescent microscope.

Matrigel plug assay.

Matrigel (0.5 mL/plug) were injected s.c. in the midventral abdominal region of 4-6 week-old C57BL/6 mice (four mice for each group). The next day mice were injected i.v. by vehicle or barbigerone every 2 days for 4 times. After treatment, the mice were sacrificed and the plugs were moved. The Matrigel plugs were fixed with 10% formalin and embedded with paraffin. The 5-μm sections were stained with H&E staining. The number of blood vessels in 200× high power field was counted.

In vivo analysis of tumor growth and lung metastasis

For tumor growth experiment, approximately 5.0×10^5 B16F10 cells in 50 μL serum-free medium were implanted subcutaneously on female C57BL/6 mice (4-6 week old, one tumor per mouse, n = 7 mice per group). After tumor volume reached 100mm3 mice were divided randomly into four groups and were treated by i.v. injection of either barbigerone (5, 10, 15 mg/kg) or vehicle every two days for 7 times. Tumor volume was observed. Tumor size was determined by measuring of the largest and perpendicular diameters every three days. Tumor volume was calculated according to the formula $V = length \times width^2 \times 0.52$.

In the metastasis study, female C57BL/6 mice (4-6 week old, n = 7 mice per group) were injected i.v. with 2.0×10^5 B16F10 cells in 50 μL serum-free medium. From the second day of implant, 7.5 mg/kg, 15 mg/kg of barbigerone and vehicle were injected i.v. into the tail vein of the mice every 2 days for 7 times.

After mice were sacrificed, tumors, some internal organs including the lungs were collected. Tumors and tissues were excised and fixed in 10% formalin for further histologic analysis. All animals used in the experiments were treated humanely in accordance with Institutional Animal Care and Use Committee guidelines.

Histologic analysis

Tumors and tissues were fixed in 10% neutral buffered formalin solution and embedded in paraffin. Sections 3-5 μm of lungs and other tissues were stained with hematoxylin and eosin (H&E). The immunohistochemistry staining of tumors was performed as follows: tumors of each group were fixed in 4% paraformaldehyde, dehydrated and embedded in paraffin. Rat anti-mouse CD31 used for immunohistochemistry were applied to paraffin-embedded material following antigen retrieval (high-pressure). Immuno-reactivity was visualized using peroxidase-DAB. Microvessel counting was done at ×200. The results regarding angiogenesis were expressed as the percentage of the micro-vessel per high-power field of three sections in each tumor compared with control.

Statistical analysis

All data were analyzed using SPSS 13.0. Statistical comparisons were made with one-factor analysis of variance (ANOVA) and a two-tailed t test. Results are presented as means ± SD. In all statistical analysis, *P*<0.05 was taken as significant. Experiments were performed at least in triplicate.

Results

*Barbigerone inhibits B16F10 cell proliferation, migration, actin assemble, invasion and induces apoptosis **in vitro***

Tumor growth and metastasis are correlated to a series of complex cell proceeding including cell proliferation, migration and invasion. If one or several of the steps are interrupted, tumor growth or metastasis may be influenced. MTT assay was used to investigate the anti-proliferation effect of barbigerone on B16F10 cells. B16F10 cells were treated with barbigerone at different concentrations
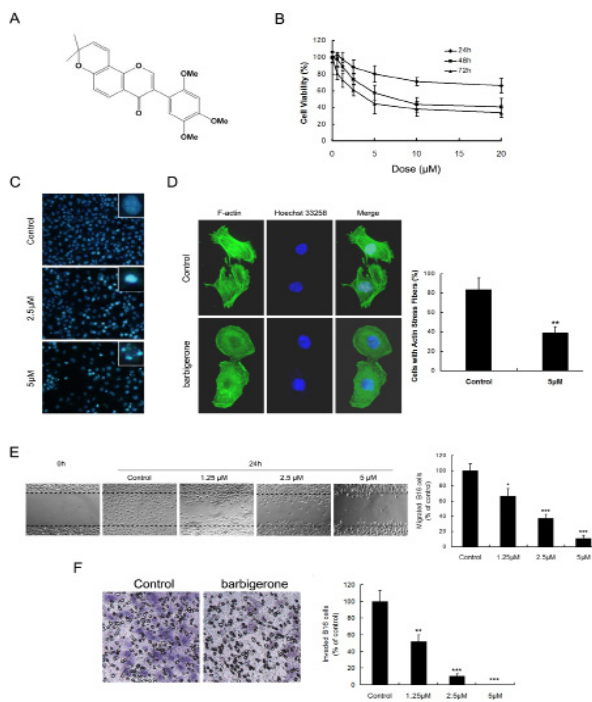
Figure 1. Barbigerone Inhibits B16F10 Cell Migration, Actin Assemble, Invasion and Induce Apoptosis *in Vitro*. (A) Structure of barbigerone. (B) MTT assay. Viability changes of B16F10 cells exposed to various concentrations 0, 0.625 μM, 1.25 μM, 2.5 μM, 5 μM, 10 μM and 20 μM for 24h, 48h and 72 h, respectively. Viability of control cells was considered as 100%. (C) Morphological analysis of apoptosis hoechst 33258 staining. Blebbing and condensation of nucleus were observed in 2.5 μM and 5 μM barbigerone treated cells, indicating barbigerone induced apoptosis of B16F10 cells. (D) F-actin stress fibers formation measured by green fluorescent phalloidin staining. In 5 μM barbigerone treated group, cells with actin stress fibers present amount of 39% which is about the half of control (84%). (E) Wound-healing assay. B16F10 cells were scraped with a sharp edge to make a cell-free area (0 hr). Cells were cultured in the presence of 0, 1.25 μM, 2.5 μM, 5 μM barbigerone for 24h and photographed. (F) Transwell invasion assay. The 8μm transwell chambers were coated with Matrigel and then seeded B16F10 cells (5×10^4 per well, with or without barbigerone) for 16h to let them go through the membrane. The blue cells in the images were invaded cells attached on outside surface of the top chamber. Five μM barbigerone inhibited almost all invasion activities of B16F10 cells. Data are expressed as mean±SD. *$p<0.05$ vs. control, **$p<0.01$ vs. control, ***$p < 0.001$ vs. control

for 24h, 48h and 72 h, respectively. As shown in Figure 1B, barbigerone potently inhibited B16F10 tumor cell proliferation both in dose- and time- dependent manners. Exposure to barbigerone at 1.25μM for 48 h caused an 11% cell growth inhibition and further resulted in the inhibition of 57% at 10μM. Five μM barbigerone resulted in an inhibition of 20% in 24h treatment and 55% in 72h treatment.

B16F10 cells were examined under a fluorescence microscopy after staining with Hoechst 33258 for morphological analysis of apoptosis. Treatment over 48h of B16F10 cells resulted in some morphological changes characteristic for apoptosis: a brightly blue-fluorescent condensed (integrity or fragmented) by fluorescence microscopy of Hoechst-stained nuclei, blebbing, reduction
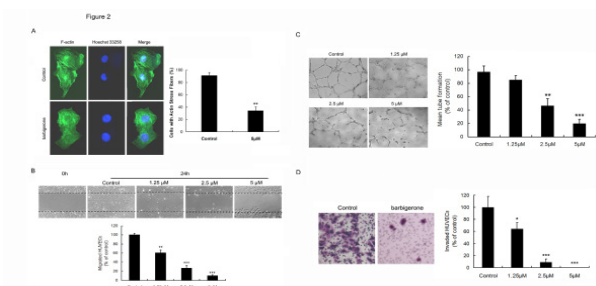

Figure 2. Barbigerone Inhibits HUVECs Migration, Actin Assemble, Invasion and Tube Formation *in Vitro*. (A) F-actin stress fibers formation measured by green fluorescent phalloidin staining. The percentage of cells with actin stress fibers decreased from 91% to 34%. (B) Wound-healing assay. Quantitative of migration cells treated by 0, 1.25 μM, 2.5 μM, 5 μM barbigerone for 24 h. (C) Tube formation assay. HUVECs were suspended in regular medium in the absence or presence of different concentrations of barbigerone and carefully layered on the top of polymerized Matrigel. All tube formation experiments were taken images at 6 h after plating. Evaluation of mean tube formation showed that 2.5 μM barbigerone inhibited approximately 50% and further 5 μM barbigerone could suppress 80% tube formation of HUVECs. (D) Transwell invasion assay. Five μM barbigerone inhibited almost all invasion activities of HUVECs. Data are expressed as mean±SD. *$p<0.05$ vs. control, **$p<0.01$ vs. control, ***$p < 0.001$ vs. control

of cell volume, condensation of nuclear chromatin, nuclear fragmentation and apoptotic bodies (Figure 1C).

The capability of cancer cell migration is contributed to the spread of metastatic tumor cells to distant organs (Gupta et al., 2006). The migration abilities of B16F10 were examined by the wound healing assay. After 24h of culture, barbigerone showed prominent effects on the migration of B16F10 cells, with significant inhibition even at the concentration of 1.25μM (Figure 1E, p<0.05). Five μM barbigerone treated for 24 h resulted in an 89% inhibition of wound closure compared with control cultures, which were considered as resulting in 100% wound closure (Figure 1E, p < 0.001), indicating that barbigerone showed a remarkably inhibitory to B16F10 cells migration.

F-actin is at least in part responsible for shaping cell morphology as well as regulating cell migration. Cell migration appears to be tightly correlated to actin assembly (Small et al., 1998). Cells with dysregulated F-actin formation have defects in their migration abilities (Olson et al., 2009). Therefore, we tested whether barbigerone could affect cell actin cytoskeleton formation by using fluorescent phalloidin staining. The results in Figure 1D showed barbigerone treated B16F10 cells had an insufficient F-actin cytoskeleton formation. In 5μM barbigerone treated group, cells with actin stress fibers presented amount of 39% which was only the half of control (84%) (Figure 1D, p<0.01).

Invasion is also one of the key steps of tumor metastasis. We performed transwell assays to evaluate the ability of B16F10 to pass through the membrane barrier of the transwell in the presence of barbigerone. As shown in Figure 1F, 2.5μM barbigerone present a 90% inhibition of B16F10 cells and 5μM barbigerone inhibited almost all invasion activities of B16F10 (p<0.001), suggesting that
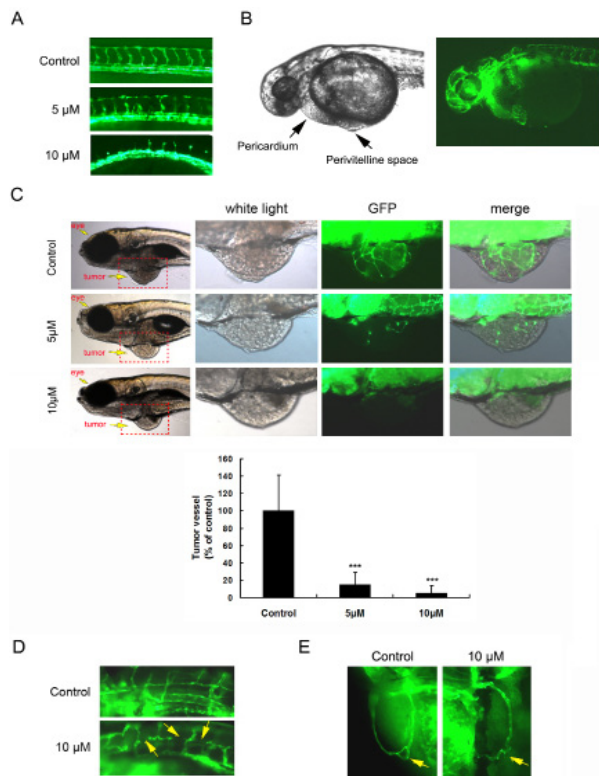
Figure 3. Barbigerone Inhibits Angiogenesis and Tumor Angiogenesis on Zebrafish Model. (A) Barbigerone was added into the culture fluid of Flk-1-GFP transgenic zebrafish embryo at 10 hours post-fertilization (hpf). Both 5μM and 10μM barbigerone significantly inhibited the trunk intersomite vessels and dorsal longitudinal anastomotic vessels after 30hpf. (B) B16F10 cells were injected in the perivitelline space at 72 hpf. Each group was treated with or without barbigerone at 96 hpf. (C) After B16F10 tumor model established on zebrafish embryos, high-density vasoganglions were induced by control group tumors while only scattered, short or fragmentary blood vessel were grown in barbigerone administration group. Tumor vessel lenth was inhibited more than 80% and 90% in 5μM and 10μM barbigerone treated group, respectively. (D) 10μM barbigerone inhibited the formation of dorsal anastomotic vessels after 216hpf. (E) 10μM barbigerone also disturbed the formation of vessel annulation in fins. Data are expressed as mean±SD. ***p<0.001 vs. control

barbigerone notably inhibited the invasion properties of B16F10 cells at low concentrations.

*Barbigerone inhibits HUVECs migration, actin assemble, invasion and tube formation **in vitro***

As cell migration and invasion are two critical aspects for endothelial cells to form new blood vessels during angiogenesis processes, we performed wound-healing assay and invasion assays to determine the effects of barbigerone on HUVEC migration and invasion. Barbigerone also inhibited the migration (Figure 2B) and invasion (Figure 2D) of HUVECs in a dose-dependent manner. Expose to barbigerone at respective concentrations of 2.5μM and 5μM strongly inhibited the migration and invasion of HUVECs (Figure 2B, 2D, p<0.001). The percentage of cells with actin stress fibers also decreased from 91% to 34% (Figure 2A, p<0.01).

Although angiogenesis is a very complex process, tube formation of endothelial cells is the key step (Patan et al.,

2004). To examine the potential effects of barbigerone on the tubular structure formation of endothelial cells, we added different concentrations of barbigerone onto matrigel and examined the formation of cord-like structure of HUVECs (Figure 2C). Our results showed that 2.5μM barbigerone inhibited approximately 50% and further 5μM barbigerone could suppress 80% tube formation of HUVECs on Matrigel assay, suggesting barbigerone is a potential potent inhibitor of angiogenesis.

Barbigerone inhibits angiogenesis and tumor angiogenesis on zebrafish model

The first experiment was performed to investigate the anti-angiogenesis effect of barbigerone on newly born Flk-1-GFP transgenic zebrafish embryos. Barbigerone significantly inhibited the blood vessel development in the trunk region. Trunk intersomite vessels and dorsal longitudinal anastomotic vessels were incomplete and with weak green fluorescent protein (GFP) fluorescence in 5μM barbigerone treated group. Furthermore, embryos given the dose of 10μM exhibited a complete inhibition of dorsal longitudinal anastomotic vessels (Figure 3A).

The main aim of the second study was to measure the influence of barbigerone on tumor-induced angiogenesis in Flk-1-GFP transgenic zebrafish embryos. After B16F10 tumor model established on zebrafish embryos, high-density vasoganglions were clearly observed in control group. In contrast, only scattered or fragmentary blood vessels were grown in barbigerone-treated zebrafish model (Figure 3C). Treatment with 10μM barbigerone resulted in 90% inhibition of blood vessel (Figure 3C, p<0.001). Meanwhile, 10μM barbigerone caused non-anastomotic dorsal vessels (Figure 3D) and also disturbed the formation of vessel annulation in fins (Figure 3E) after 216hpf.

Barbigerone inhibits tumor angiogenesis and tumor growth on mouse model

Tumor angiogenesis provides oxygen, nutrition, passage for tumor cell spreading and main routes for tumor growth, invasiveness, and metastasis and acts as a rate-limiting step in tumor progression (Tozer et al., 2005). To analyze the inhibitory effects of barbigerone on angiogenesis *in vivo*, we performed the mouse Matrigel plug assay. As shown in Figure 4A, 15mg/kg barbigerone inhibited more than 70% vessel growth in Matrigel plug, indicating barbigerone strongly inhibited angiogenesis *in vivo*.

To further determine the effect of barbigerone on tumor angiogenesis and tumor growth at nontoxic dosage, we used B16F10 tumor-bearing mice as describing in Materials and Methods. Barbigerone effectively prevented the tumor growth in both volume and weight in a dose-dependent manner. After 14 days of initiate administration, mean tumor volume in 15mg/kg barbigerone treated mice was 1082.6±183.2 mm3 versus 4010.9±257.1 mm3 in control group (Figure 4B, *p*<0.001), with 73% inhibiting rate of tumor volume. Barbigerone-treated mice showed significantly lower tumor weights and size at the end of experiment (Figure 4B, *p* < 0.01). The results demonstrated that barbigerone was effective to inhibit growth of tumors on B16F10 tumor-bearing mice.
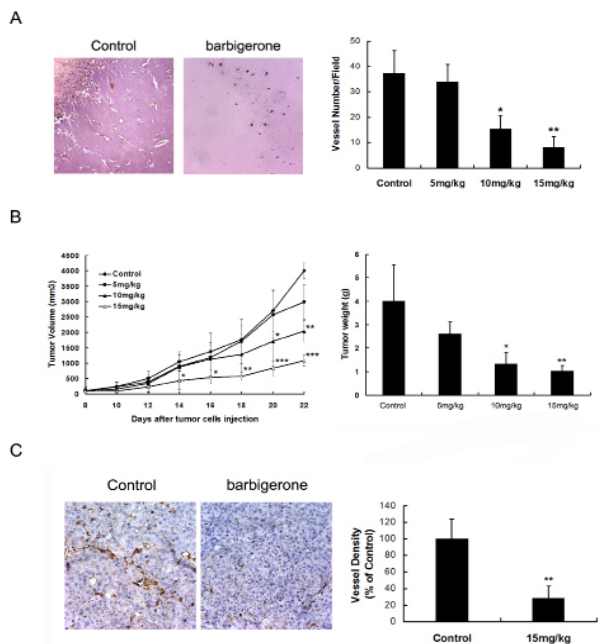
Figure 4. Barbigerone Inhibits Tumor Angiogenesis and Tumor Growth on Mouse Model. (A) Matrigel plug assay. Matrigel (0.5 mL/plug) were injected s.c. in 4-6 week-old C57BL/6 mice. Then mice were treated by vehicle or barbigerone every 2 days for 4 times. The Matrigel plugs were embedded with paraffin. The 5-μm sections were stained with H&E staining. The number of blood vessels in 200× high power field was counted, 15 mg/kg barbigerone inhibited more than 70% vessel growth in Matrigel plug. (B) For tumor growth study, 5.0×10^5 B16F10 cells were implanted subcutaneously on female C57BL/6 mice (4-6 week old, n = 7 mice per group). Mice were treated by i.v. injection of either barbigerone (5, 10, 15 mg/kg) or vehicle every two days for 7 times. At the 14 day after administration, mean tumor volume in 15mg/kg barbigerone treated mice was 1082.6±183.2 mm3 versus 4010.9±257.1 mm3 in control group. Barbigerone-treated mice showed significantly lower tumor weights. (C) Microvessel in tumors was stained by CD31. Fifteen mg/kg barbigerone resulted in a significant reduction of tumor vessels compared with control. Barbigerone-treated tumors had nearly decreased 70% of tumor microvessel amount versus control group. Data are expressed as mean±SD. *p<0.05 vs. control, **p<0.01 vs. control, ***$p < 0.001$ vs. control

Microvessel density was quantified to measure angiogenesis by immunolabeling of CD31 in solid tumor sections. Administration of 15mg/kg barbigerone resulted in the apparent reduce of tumor vessels in B16F10 tumors compared with the control therapy. Barbigerone-treated tumors had nearly decreased 70% of tumor microvessel amount versus control group (Figure 4C, p<0.01).

Barbigerone suppresses lung metastasis

To determine whether barbigerone could suppress the growth of tumor metastases, we established mice lung metastasis model by i.v. injection of 2.0×10^5 B16F10 cells in female C57BL/6 mice (4-6 week old, n = 7 mice per group). Gross examination revealed numerous lung surface metastases in the control group. In contrast, there were fewer visible lung surface metastases in barbigerone-treated mice (Figure 5A).

Comparison of tumor metastasis by counting the lung surface metastases confirmed that mice in control group
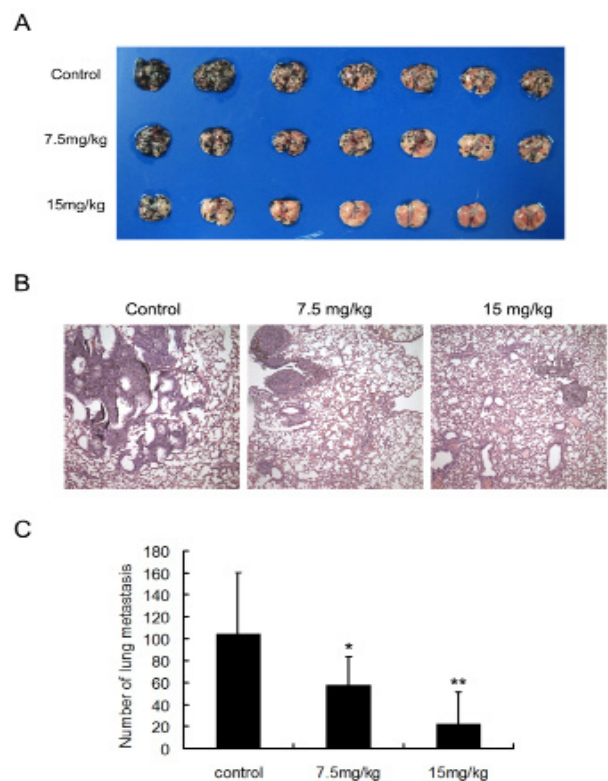
Figure 5. Barbigerone Suppresses Lung Metastasis. 2.0×10^5 B16F10 cells were i.v. injected in female C57BL/6 mice (4-6 week old, n = 7 mice per group). (A) Numerous lung surface metastases visible in the control group whereas there were fewer lung surface metastases in barbigerone-treated mice. (B) H&E staining of lung sections presented numerous large metastases in lungs from control mice whereas only small, avascular metastases could be seen in lungs from barbigerone-treated mice. (C) Number of lung surface metastases of control group was 104.3±55.9, which was approximately 2-fold of 7.5 mg/kg barbigerone group (57.1±26.1) and 5-fold of 15 mg/kg barbigerone group (22.5±28.8), respectively. Data are expressed as mean±SD. *p<0.05 vs. control, **p<0.01 vs. control

carried a significantly greater metastatic burden than mice treated with barbigerone (Figure 5C). Number of lung surface metastases of control group was 104.3±55.9, which was approximately 2-fold of 7.5mg/kg barbigerone group (57.1±26.1, p<0.05) and 5-fold of 15mg/kg barbigerone group (22.5±28.8, p<0.01), respectively.

Histologic examination of H&E-stained lung sections presented numerous large metastases in lungs from control mice whereas only small, avascular metastases could be seen in lungs from barbigerone-treated mice (Figure 5B).

Barbigerone inhibits p38 MAPK signaling pathway

Because mitogen-activated protein kinase (MAPK) pathways can influence various processes of tumor cells proliferation, survival and migration, we detected three major groups of MAPK including p44/p42 MAPKs (ERK1/2), c-Jun aminoterminal kinases (JNK1/2) and p38 MAPKs to detect the effect of barbigerone on MAPK signaling pathways. As shown in Figure 6A, 5μM barbigerone could remarkably inhibit the phosphorylation of ERK1/2 and JNK1/2 in B16F10 cells. We also detected Akt which is also an important factor in regulation of multiple critical steps in tumor
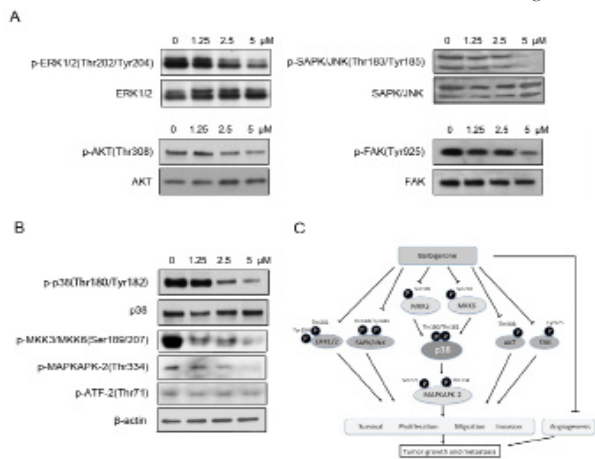
Barbigerone Inhibits Tumor Angiogenesis, Growth and Metastasis in Melanoma

Figure 6. Barbigerone Inhibits p38 MAPK Signaling Pathway. B16F10 cells were cultured in DMEM media containing various concentrations of barbigerone (0, 1.25, 2.5 or 5 μM) for 16 h, and then the cell lysates were subjected to SDS-PAGE followed by western blots with total and phosphorylated antibodies. A, Barbigerone could inhibit the phosphorylation of ERK1/2, JNK1/2 and FAK in B16F10 cells. Slightly influence the phosphorylation of AKT. B, Barbigerone could remarkably inhibit the activity of phospho-p38 via suppressing the phosphorylation of both MKK3 and MKK6 and further inactivate the expression of downstream factor p-MAPKAPK-2, but not affect p-ATF-2. C, Diagram of signaling pathways for barbigerone-mediated anti-tumor angiogenesis, tumor growth and metastasis. Barbigerone can interfere tumor cell survival, proliferation, migration and invasion via downregulating p38 MAPK pathway

cell proceeding. Influence of the phosphorylation of AKT was also visible in barbigerone treated B16F10 cell. We further text some of the important kinases from p38 MAPK pathway. Barbigerone could inhibit the activity of phospho-p38 via suppressing the phosphorylation of both MKK3 and MKK6 and further inactivate the expression of downstream factor p-MAPKAPK-2, but not affect p-ATF-2 (Figure 6B).

The focal adhesion complex is one of the important components promoting cell motility. We evaluated the effects of barbigerone on the formation of focal adhesion complexes by examining the levels of tyrosine phosphorylations of FAK, which was one of the elementary proteins for forming stable adhesion complexes and transducing the survival/migration signals. After 16h-treatment of 0-5μM barbigerone on B16F10 cells, the ratio of phosphorylated FAK/FAK was decreased in a concentration-dependent manner (Figure 6A).

Discussion

The major cause of cancer mortality is the metastatic spread of tumor cells that can occur via blood vasculature (Zhang et al., 2010). Because tumor growth and metastasis depend on tumor angiogenesis, inhibition of tumor angiogenesis is a novel therapeutic modality toward controlling tumor metastasis (Kruger et al., 2001). Angiogenesis is initiated by endothelial cell proliferation, migration, invasion and then tube formation (Fan et al., 2006). It has been shown that suppression at any step of the processes in angiogenesis will inhibit the formation of

new blood vessels (Tournaire et al., 2004). In our present study, we demonstrate that barbigerone inhibits HUVECs migration, actin assemble, invasion and tube formation *in vitro* in the dose-dependent manner. Treatment of 5 μM barbigerone resulted in a 90% inhibition of wound closure and 80% inhibition of tube formation compared with control, respectively. The concentration of 5 μM barbigerone exhibited a completely inhibition of invade HUVECs. The percentage of cells with actin stress fibers also decreased from 91% to 34%. We further used two animal models (transgenic zebrafish and C57BL/6 mice) to investigate whether barbigerone could inhibit angiogenesis *in vivo*. 10μl barbigerone to tumor vessel was inhibited 90% in tumor induced vessel in zebrafish and 15mg/kg barbigerone resulted in obvious decrease of microvessel density in mice tumor model. The results shows that barbigerone could inhibit angiogenesis and tumor induced angiogenesis both *in vitro* and *in vivo*.

Meanwhile, we evaluated the direct anti-tumor effect of barbigerone on tumor cells, barbigerone inhibited B16F10 proliferation both in time- and dose- dependent manner and induced tumor cell apoptosis in both 2.5 μM and 5 μM. In order to make sure that the inhibition of migration and invasion are not due to the cytotoxicity effect of barbigerone, we chose concentration of no more than 5 μM and treating time was no longer than 24 h. After 24 h's treatment, 5 μM of barbigerone caused only 20% inhibition of proliferation but resulted in an 89% inhibition of wound closure and inhibited almost all invasion activities of B16F10. *In vivo*, barbigerone-treated mice showed significantly lower tumor weights and tumor size at the end of experiment. Furthermore, number of lung surface metastases of 15mg/kg barbigerone group was decreased to 22.3±28.8 compared with control group (104.3±55.9). Taken together, barbigerone could not only cut off the route of oxygen and nourishment provision via interrupting tumor angiogenesis but also directly inhibit tumor cells survival, proliferation, migration and invasion.

Mitogen-activated protein kinase pathways mediated by ERK, JNK, and p38 protein. MAPK pathway can influence tumor cells proliferation, survival and migration. The results of Western bolt indicated barbigerone could inhibit the phosphorylation of ERK1/2, JNK1/2 and p38 in B16F10 cells and also affect phosphorylation of AKT. FAK signaling was shown to promote invasive behavior of cells through a pathway involving JNK-mediated transcriptional activation of MMP-2 and MMP-9 pathway (Hsia et al., 2003). Barbigerone can also decrease the ratio of phosphorylated FAK/FAK which is concerned with cell migration in a dose-dependent manner. MKK3 and MKK6 activate p38 MAP kinase by phosphorylation at Thr180 and Tyr182. Activated p38 MAP kinase has been shown to phosphorylate and activate MAPKAP kinase 2 (Lee et al., 1994) and to phosphorylate the transcription factors ATF-2 (Raingeaud et al., 1995). Our data shows that barbigerone could strongly inhibit the activity of phospho-p38 via suppressing the phosphorylation of both MKK3 and MKK6 and further inactivate the expression of downstream factor p-MAPKAPK-2, but not affect p-ATF-2.

Our study has shown for the first time that barbigerone

exhibits the capability of suppressing tumor angiogenesis, tumor growth and metastasis. For anti-angiogenesis ability, barbigerone (i) inhibits migration and interferes the formation of cytoskeleton of HUVECs; (ii) suppresses HUVECs invasion; (iii) inhibits HUVECs tube formation; (iv) restrains both angiogenesis and tumor-associated angiogenesis. Moreover, barbigerone displays the role of inhibiting tumor growth and metastasis, barbigerone (i) inhibits proliferation, migration and interferes the formation of cytoskeleton of tumor cells; (ii) induces apoptosis of tumor cells; (iii) suppresses invasion of tumor cells; (iv) restrains tumor growth and lung metastasis (v) down-regulates the expression of phosphorylation of ERK1/2, JNK1/2, p38, AKT and FAK in tumor cells.

In summary, our results indicate that barbigerone significantly inhibits angiogenesis, tumor growth and metastasis *in vitro* and *in vivo* by suppressing cell proliferation, migration, invasion and survival through p38 MAPK signaling pathway. Our findings suggest that barbigerone could be further explored as a promising therapeutic agent against angiogenesis, tumor growth and metastasis.

Acknowledgements

References

Amundadottir LT, Leder P (1998). Signal transduction pathways activated and required for mammary carcinogenesis in response to specific oncogenes. *Oncogene*, **16**, 737-46.

Carmeliet P (2003). Angiogenesis in health and disease. *Nat Med*, **9**, 653-60.

Carmeliet P, Base M (2008). Metabolism and therapeutic angiogenesis. *N Engl J Med*, **358**, 2511-2.

Carmeliet P, Jain RK (2000). Angiogenesis in cancer and other diseases. *Nature*, **407**, 249-57.

Davidson B, Konstantinovsky S, Kleinberg L, et al (2006). The mitogen-activated protein kinases (MAPK). p38 and JNK are markers of tumor progression in breast carcinoma. *Gynecol Oncol*, **102**, 453-61.

Fan TP, Yeh JC, Leung KW, Yue PY, Wong RN (2006). Angiogenesis: from plants to blood vessels. *Trends Pharmacol Sci*, **27**, 297-309.

Ferrara N, Kerbel RS (2005). Angiogenesis as a therapeutic target. *Nature*, **438**, 967-74.

Folkman J (1971). Tumor angiogenesis: therapeutic implications. *N Engl J Med*, **285**, 1182-6.

Folkman J, Shing Y (1992). Angiogenesis. *J Biol Chem*, **267**, 10931-4.

Gupta GP, Massague J (2006). Cancer metastasis: building a framework. *Cell*, **127**, 679-95.

Johnson GL, Lapadat R (2002). Mitogen-activated protein kinase pathways mediated by ERK, JNK, and p38 protein kinases. *Science*, **298**, 1911-2.

Hsia DA, Mitra SK, Hauck CR, et al (2003). Differential regulation of cell motility and invasion by FAK. *J Cell Biol*, **160**, 753-67.

Huang D, Ding Y, Luo WM, et al (2008). Inhibition of MAPK Kinase signaling pathways suppressed renal cell carcinoma growth and angiogenesis *in vivo*. *Cancer Res*, **68**, 81-8.

Kruger EA, Duray PH, Price DK, Pluda JM, Figg WD (2001).

Approaches to preclinical screening of antiangiogenic agents. *Semin Oncol*, **28**, 570-6.

Lee JC, Laydon JT, Mcdonnell PC, et al (1994). A protein kinase involved in the regulation of inflammatory cytokine biosynthesis. *Nature*, **372**, 739-46.

Li X, Wang X, Ye H, Peng A, Chen L (2012). Barbigerone, an isoflavone, inhibits tumor angiogenesis and human non-small-cell lung cancer xenografts growth through VEGFR2 signaling pathways.*Cancer Chemother Pharmacol*, **70**, 425-37.

Olson MF, Sahai E (2009). The actin cytoskeleton in cancer cell motility. *Clin Exp Metastasis*, **26**, 273-87.

Patan S (2004). Vasculogenesis and angiogenesis. *Cancer Treat Res*, **117**, 3-32.

Raingeaud J, Gupta S, Rogers JS, et al (1995). Pro-inflammatory cytokines and environmental stress cause p38 mitogen-activated protein kinase activation by dual phosphorylation on tyrosine and threonine. *J. Biol. Chem*, **31**, **270**, 7420-6.

Reddy KB, Nabha SM, Atanaskova N (2003). Role of MAP kinase in tumor progression and invasion. *Cancer Metastasis Rev*, **22**, 395-403.

Small JV, Rottner K, Kaverina I, Anderson KI (1998). Assembling an actin cytoskeleton for cell attachment and movement. *Biochim Biophys Acta*, **1404**, 271-81.

Tournaire R, Simon MP, le Noble F, et al (2004). A short synthetic peptide inhibits signal transduction, migration and angiogenesis mediated by Tie2 receptor. *EMBO Rep*, **5**, 262-7.

Tozer GM, Kanthou C, Baguley BC (2005). Disrupting tumor blood vessels. *Nat Rev Cancer*, **5**, 423-35.

Uzgare AR, Kaplan PJ, Greenberg NM (2003). Differential expression and/or activation of P38MAPK, erk1/2, and jnk during the initiation and progression of prostate cancer. *Prostate*, **55**, 128-39.

Vicent S, Garayoa M, Lopez-Picazo JM, et al (2004). Mitogen-activated protein kinase phosphatase-1 is overexpressed in non-small cell lung cancer and is an independent predictor of outcome in patients. *Clin Cancer Res*, **10**, 3639-49.

Vilain C (1980). Barbigerone, a new pyranoisoflavone from seeds of Tephrosia barbigera. *Phytochem*, **19**, 988-9.

Wangensteen H, Alamgir M, Rajia S, Samuelsen AB, Malterud KE (2005). Rotenoids and isoflavones from Sarcolobus globosus. *Planta Med*, **71**, 754-8.

Wangensteen H, Miron A, Alamgir M, et al (2006). Antioxidant and 15-lipoxygenase inhibitory activity of rotenoids, isoflavones and phenolic glycosides from Sarcolobus globosus. *Fitoterapia*, **77**, 290-5.

Webb CP, Van Aelst L, Wigler MH, Woude GF (1998). Signaling pathways in Ras-mediated tumorigenicity and metastasis. *Proc Natl Acad Sci USA*, **95**, 8773-8.

Ye HY, Zhong SJ, Li YF, et al (2010). Enrichment and isolation of barbigerone from Millettia pachycarpa Benth. using highspeed counter-current chromatography and preparative HPLC. *J Sep Sci*, **33**, 1010-7.

Yenesew A, Derese S, Midiwo JO, Oketch-Rabah HA, Lisgarten J, Palmer R, et al (2003). Anti-plasmodial activities and X-ray crystal structures of rotenoids from Millettia usaramensis subspecies usaramensis". *Phytochem*, **64**, 773-9.

Yenesew A, Midiwo JO, Waterman PG (1998). Rotenoids, isoflavones and chalcones from the stem bark of Millettia usaramensis subspecies usaramensis. *Phytochem*, **47**, 295-300.

Zhao CJ, Yang HS, Shi HS, et al (2011). Distinct Contributions of Angiogenesis and Vascular Co-option during the Initiation of Microtumors and Micrometastases. *Carcinogenesis*, **32**, 1143-50.

Zhang D, Li B, Shi J, et al (2010). Suppression of Tumor Growth and Metastasis by Simultaneously Blocking Vascular Endothelial Growth Factor (VEGF).-A and VEGF-C with a Receptor-Immunoglobulin Fusion Protein. *Cancer Res*, **70**, 2495-503.